

SUPPORTING INFORMATION

Exceptionally high Sodium-ion Battery Cathode Capacity-Based on Doped Ammonium Vanadium Oxide and Full Cell SIB Prototype Study

*Ananta Sarkar, Sudeep Sarkar and Sagar Mitra**

Electrochemical Energy Laboratory, Department of Energy Science and Engineering,

Indian Institute of Technology Bombay, Powai, Mumbai-400076, Maharashtra, India

Tel: + 91-222576-7849. E-mail: sagar.mitra@iitb.ac.in

Experimental section

Synthesis of Cathode:

Zirconium doped ammonium vanadium oxide, $\text{Zr-NH}_4\text{V}_4\text{O}_{10}$ a one-directional nano-belts were prepared by modified hydrothermal synthesis process as discussed in our previous report.¹ In a typical synthesis, the exact amount of vanadium oxide (V) (V_2O_5 , Sigma Aldrich, 99.6%) was added to 10 mL of ammonium hydroxide solution (NH_4OH , Merck India, 30%) and the yellow color V_2O_5 of the mixture changed from yellow to white. Later, this mixture was added to 70 mL of oxalic acid solution (0.1 M) (Fisher Scientific, 99.5%) and continuously stirring for 20 min. In addition zirconium (IV) hydroxide (Aldrich 97%) was added to the same solution at different mole ratio of V:Zr = 10:1, 15:1, 20:1,30:1 and 40:1. The pH of the solution was kept constant ~ 3, by dropwise adding hydrochloric acid (HCl, Merck, 37%). Later, the solution was transferred into 100 mL Teflon lined autoclave and heated at 190 °C for 5 h to get desired shape and size. The final product was collected by centrifugation and washing with de-ionized (DI) water several times and dried at 60 ± 5 °C overnight in a vacuum oven.

Synthesis of Anode:

Hydrogenated sodium titanium oxide ($\text{Na}_2\text{Ti}_3\text{O}_7$) nanorods were prepared by simple hydrothermal process followed by hydroxide treatment. In a typical synthesis process, 0.8 g of titanium nanopowder (Alfa Aesar, 325 mesh 99%) was added to the 70 mL of 10 M sodium hydroxide (NaOH , Fisher Scientific 97%) solution with continuous stirring, the homogeneous solution was transferred into 100 mL Teflon lined autoclave and heated at 220 °C for 6 h to obtain desired product. Finally, white $\text{Na}_2\text{Ti}_3\text{O}_7$ power was obtained after washing the materials several times with de-ionized water (DI). The final hydrogenated $\text{Na}_2\text{Ti}_3\text{O}_7$ nanorods were

collected after annealing at 450 °C for 3 h at a mixture of Ar/H₂ (90:10) atmosphere with a heating rate of 2 °C min⁻¹.

Materials Characterization:

X-ray diffraction (XRD) technique was used to characterize the crystalline structure and phase of the electrode materials systematically at room temperature using Rigaku Smartlab X-ray diffractometer with Cu K α radiation ($\lambda = 1.5418 \text{ \AA}$). Morphology of the materials analyzed by field emission gun scanning electron microscope (FEG-SEM), Carl Zeiss Ultra-55 model with a resolution about 0.8 nm. Field emission gun transmission electron microscope (FEG-TEM) also used to identify the microstructure and particles size distribution using JEM-2100F model. The oxidation states of vanadium and zirconium, as well as titanium, were confirmed by X-ray photoelectron spectroscopy (XPS, AXIS Supra, Kratos SHIMADZU Analytical) with the emission current of 15 mA and XPS data are fitted by magic plot software. Raman spectroscopy was used to analyze the materials before and after the hydrogenation of Na₂Ti₃O₇ (Horiba JobinYvonLabRAM HR 800 Duel Microscope).

Electrochemical Characterization:

The electrode was prepared by mixing of zirconium doped NH₄V₄O₁₀ or hydrogenated Na₂Ti₃O₇ as active materials, carbon black (Super C-65, Timcal, Switzerland) and carboxymethyl cellulose sodium salt (CMC, Loba-Chemie) in the weight ratio of 7:2:1, respectively. An appropriate amount of water (as a solvent) was added to the mixture and stirred to get a homogenous and thick slurry. Then the slurry was cast onto aluminum foil for cathode materials or onto copper anode materials respectively and dried at 60 \pm 5 °C in a vacuum oven overnight. Electrochemical experiments in half-cell configuration for both cathode and anode electrode vs. Na/Na⁺ were

done by using lab scale Swagelok type cells and full cell performance was analyzed using 2032 type coin cells. All type of cells was assembled inside the argon filled glovebox (Unilab Plus, Mbrun, Germany) with controlled moisture and oxygen level of 0.5 ppm. Zirconium doped ammonium vanadium oxide ($\text{Zr-NH}_4\text{V}_4\text{O}_4$) was used as a working electrode for cathode half-cell and hydrogenated $\text{Na}_2\text{Ti}_3\text{O}_7$ act as a working electrode for anode half-cell. Whereas, sodium foil pasted onto stainless steel disk used as a counter and a reference electrode in two electrode configuration for the both cases. Here, borosilicate glass microfiber filter (GF/D Whatman) used as a separator. The electrolyte was prepared by the using of 1 M sodium perchlorate (NaClO_4) salt in ethylene carbonate (EC)/ propylene carbonate (PC) (1:1 V/V) solvent. The improved the full cell electrochemical performance, pre-sodiation of cathode electrode was done. In this process, initially, cathode materials was fully cycled (1 cycle, first discharge to 1.5 V from OCV then charge to 3.7 V) then discharged up to 1.5 V completely at very slow current rate of 30 mAh g^{-1} . Then, the cell was opened inside the glove box and collected the pre-sodiated cathode materials. After that, we assembled the full cell (coin cell, 2016 type) inside the glove box (pre sodiated $\text{Zr-NH}_4\text{V}_4\text{O}_4$ electrode as cathode and $\text{H-Na}_2\text{Ti}_3\text{O}_7$ as anode). The galvanostatic charge-discharge performances were done in Arbin instrument (BT2000 model, USA) at various current and voltage range. Cyclic voltammetry (CV) experiments were carried out in Bio-Logic instrument (VMP-3 model, France) at a constant scan rate of 0.1 mV s^{-1} at various voltage ranges at a controlled temperature of $20 \pm 2 \text{ }^\circ\text{C}$ for both cathode, anode and full cell tests. Electrochemical impedance spectroscopy (EIS) study was carried out in the frequency range of 1 MHz- 100 mHz at 5mV voltage perturbation. All the electrochemical experiments were performed at $20 \pm 2 \text{ }^\circ\text{C}$, if not specified.

X-Ray Diffraction pattern (XRD) of different concentration zirconium doped ammonium vanadium oxide with corresponding JCPDS data file 031-0075 was shown in the Fig. S1e. It was noticeable that with increasing the zirconium concentration on doped Zr-NH₄V₄O₁₀ the peak intensity ratio of (001) to (110) planes is increasing. Scanning Electron Microscope (SEM) of Zr-NH₄V₄O₁₀ and pure NH₄V₄O₁₀. Cathode materials images (Fig. S1 C-d) suggested that with doping of zirconium particle size is decreased significantly. Generally Zirconium has a bigger ionic radius (86 pm) than V⁵⁺ (68 pm) which create a huge local distortion and electronic repulsion in the host and as a result, these big ions increase the bond length, expand the crystal lattice. It was observed in the literature that increase in the bond length, particle size decreases.² Fig. S1f showed that ammonium vanadium oxide with 3.33 % zirconium doping concentration (mole ratio of Zr:V = 1:30) exhibited best electrochemical performance. So, we chose 1:30 zirconium doped ammonium vanadium oxide for further experiment.

Table S1. ICP compositional analysis of as-synthesized Zr-NH₄V₄O₁₀ sample.

Element	Weight Ratio	Weight %	Mole Ratio	Mole %
V	49.168	97.80	0.9652	98.75
Zr	1.110	2.20	0.01216	1.25

Although 3.33 mole % of zirconium was added in the precursor during the preparation of Zr-NH₄V₄O₁₀, it was found from ICP analysis that the doping concentration of zirconium in vanadium site is ~ 1.25 mole %.

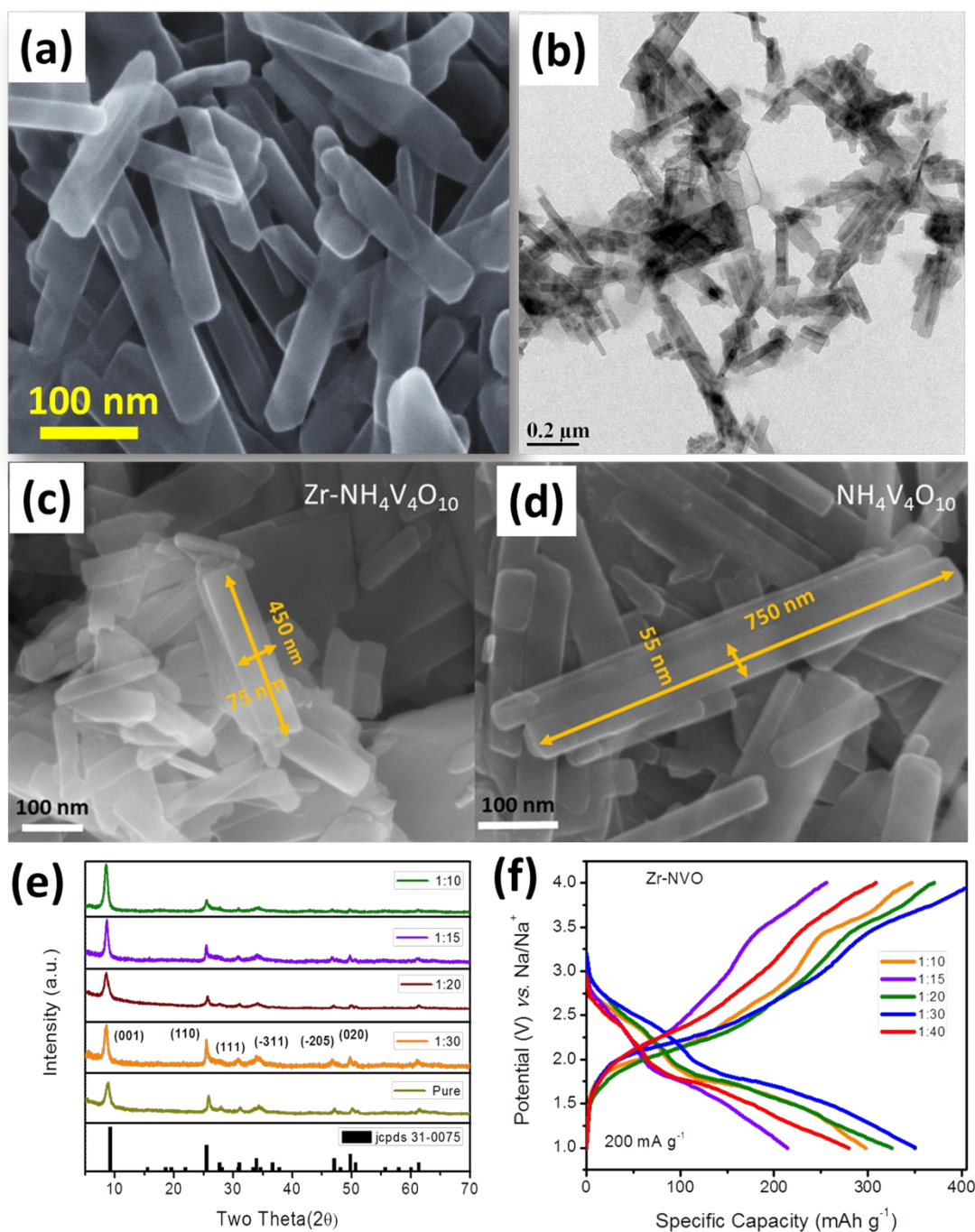


Fig. S1. Morphology analysis of $\text{Zr-NH}_4\text{V}_4\text{O}_{10}$. Cathode materials, (a) FEG-SEM images of $\text{Zr-NH}_4\text{V}_4\text{O}_{10}$, (b) FEG-TEM images of $\text{Zr-NH}_4\text{V}_4\text{O}_{10}$, FEG-SEM images of shows (c) after zirconium doping, (d) $\text{NH}_4\text{V}_4\text{O}_{10}$ particles, (e) XRD pattern of $\text{Zr-NH}_4\text{V}_4\text{O}_{10}$ at different mole ratio with corresponding JCPDS data file and (f) Optimization of electrochemical performance of $\text{Zr-NH}_4\text{V}_4\text{O}_{10}$ at different mole ratio at 200 mA g^{-1} current rate over the potential window 1-4 V.

The XPS parameters are fitted by the Gaussian and Lorentzian equation.

Gaussian - $a * \exp(-\ln(2) * (x-x_0)^2 / dx^2)$ and

Lorentzian - $a / (1 + (x-x_0)^2 / dx^2)$.

Where a is amplitude or intensity of the peaks.

Table S2. XPS Fitted Parameter

Table S2a. $\text{NH}_4\text{V}_4\text{O}_{10}$

Name	Position	FWHM	Area	Intensity
$\text{V}^{5+} 2p_{3/2}$	517.10	0.6057	6567.48	3504.69
$\text{V}^{4+} 2p_{3/2}$	515.78	0.8423	2149.21	1236.27
$\text{V} 2p_{1/2}$	524.07	1.8676	3716.90	934.85
$\text{O} 1s$	529.74	0.6930	8341.09	5653

Table S2b. $\text{Zr-NH}_4\text{V}_4\text{O}_{10}$

Name	Position	FWHM	Area	Intensity
$\text{V}^{5+} 2p_{3/2}$	517.42	0.6758	59275.04	27918.31
$\text{V}^{4+} 2p_{3/2}$	516.10	0.7812	19808.43	11910
$\text{V} 2p_{1/2}$	524.17	1.6784	29907.02	8369
$\text{O} 1s$	530.06	0.6404	68186.50	50107.14
$\text{Zr} 3d_{5/2}$	182.85	0.7648	1134.67	491.21
$\text{Zr} 3d_{3/2}$	185.05	0.7993	714.07	419.62

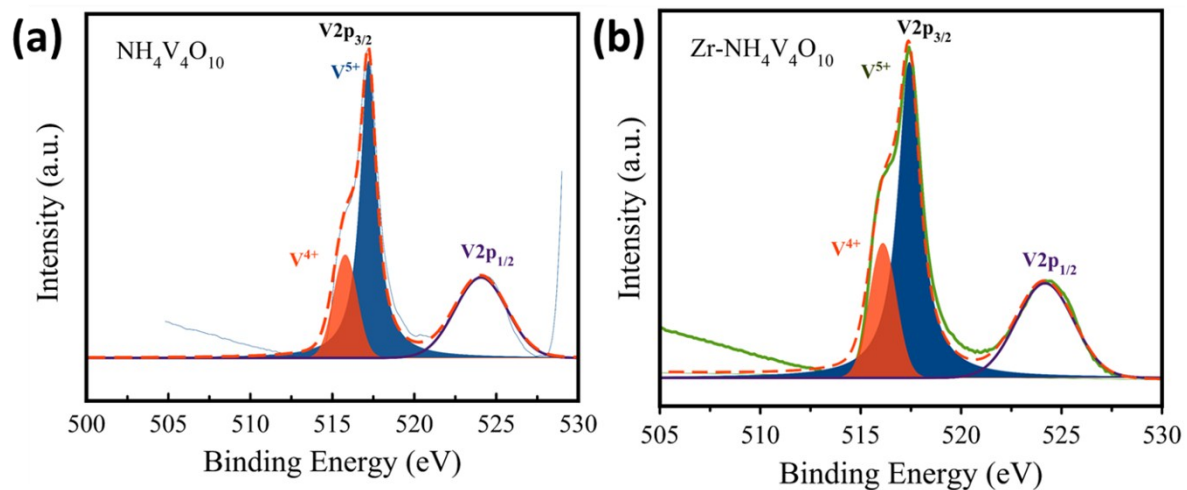


Fig. S2 X-ray photoelectron spectroscopy spectrum (XPS) spectra of vanadium for $\text{NH}_4\text{V}_4\text{O}_{10}$ and zirconium doped $\text{NH}_4\text{V}_4\text{O}_{10}$ cathode.

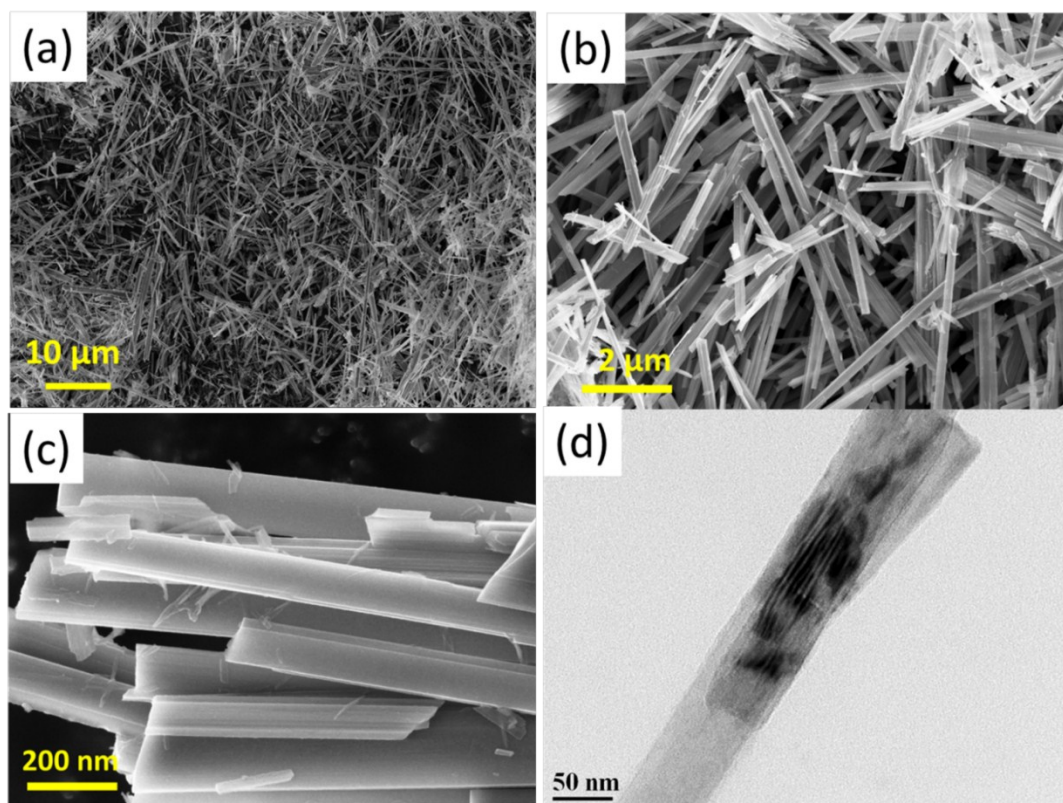


Fig. S3. (a-c) FEM- SEM image of $\text{H-Na}_2\text{Ti}_3\text{O}_7$ at different magnification and (d) FEM- TEM image of $\text{H-Na}_2\text{Ti}_3\text{O}_7$.

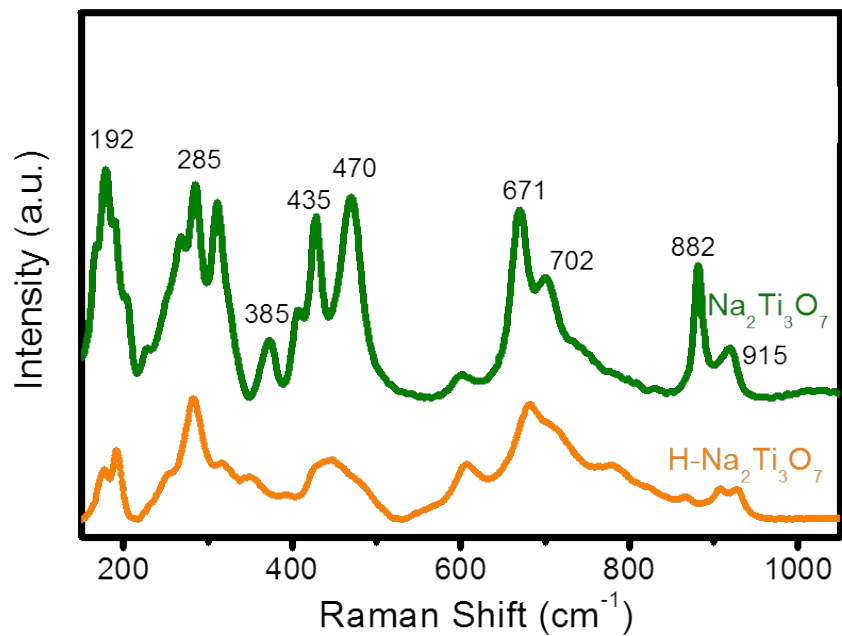


Fig. S4. Raman Spectroscopy of $\text{H-Na}_2\text{Ti}_3\text{O}_7$ and $\text{Na}_2\text{Ti}_3\text{O}_7$ as prepared sample.

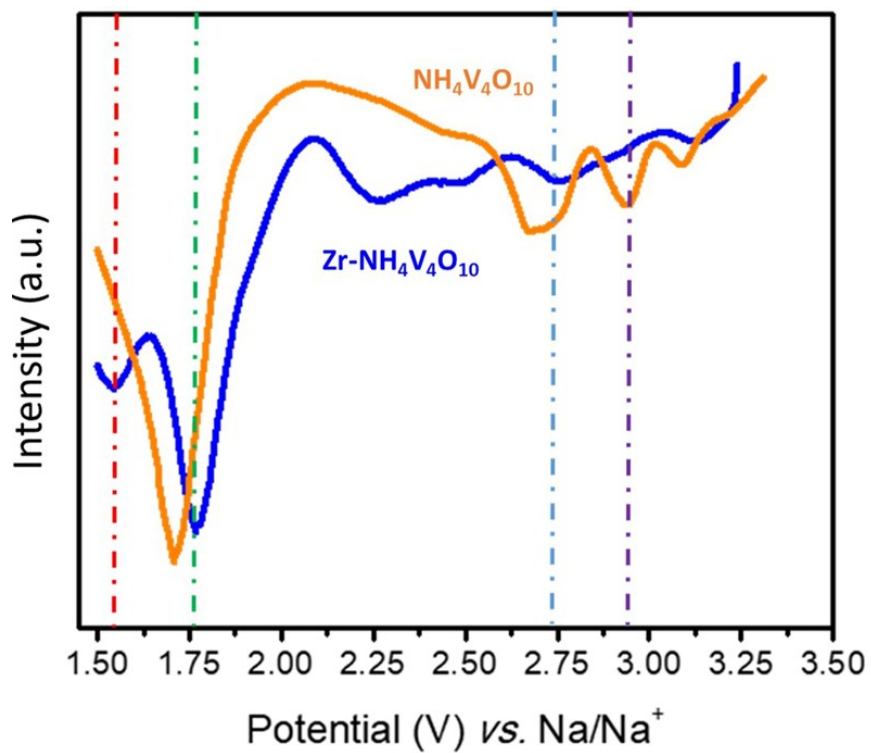


Fig. S5. 1st discharge process up to 1.5 V of $\text{NH}_4\text{V}_4\text{O}_{10}$ and $\text{Zr-NH}_4\text{V}_4\text{O}_{10}$ at 0. mV S^{-1} scan rate.

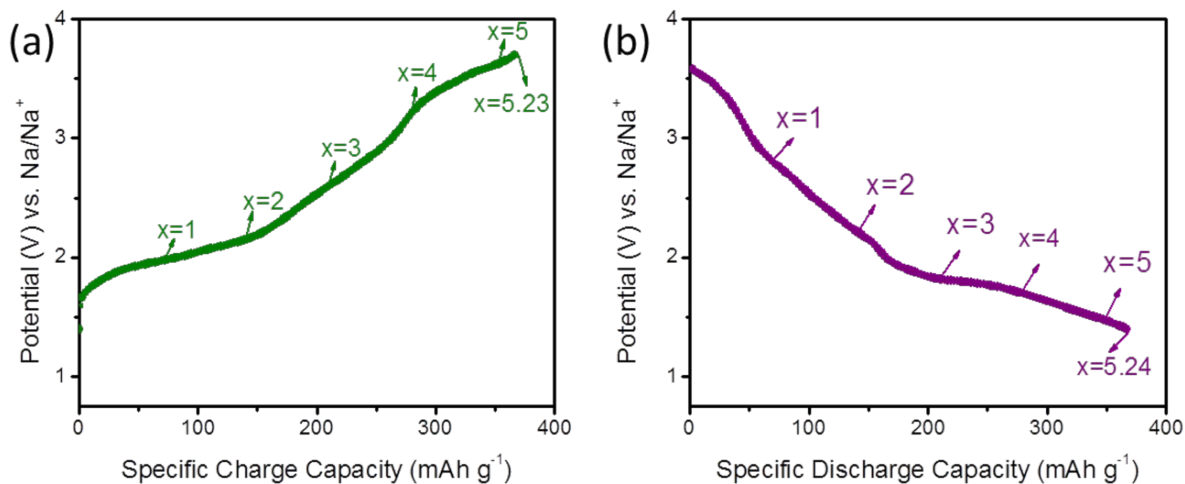


Fig. S6. No of sodium insertion/de-insertion vs. voltage profile at the current rate of 200 mA g^{-1} over 1.4-3.7 V potential window of $\text{Zr-NH}_4\text{V}_4\text{O}_{10}$ cathode materials during (a) charge process (b) discharging process.

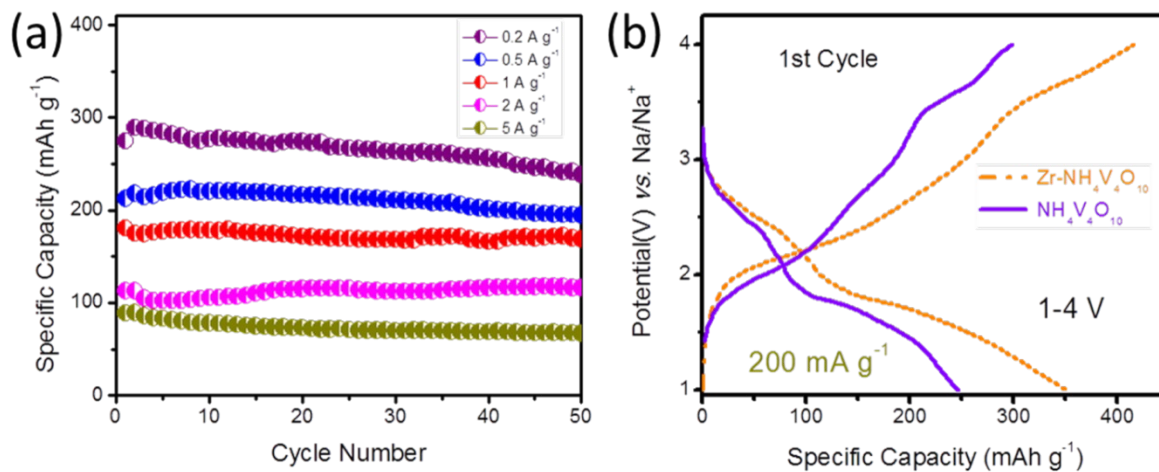


Fig. S7. (a) Discharge cycling performance at a different current rate up to 50 cycles of $\text{Zr-NH}_4\text{V}_4\text{O}_{10}$ and (b) Comparison of the electrochemical performance of $\text{Zr-NH}_4\text{V}_4\text{O}_{10}$ and $\text{NH}_4\text{V}_4\text{O}_{10}$ over the potential window 1-4V at the current rate of 200 mA g^{-1} .

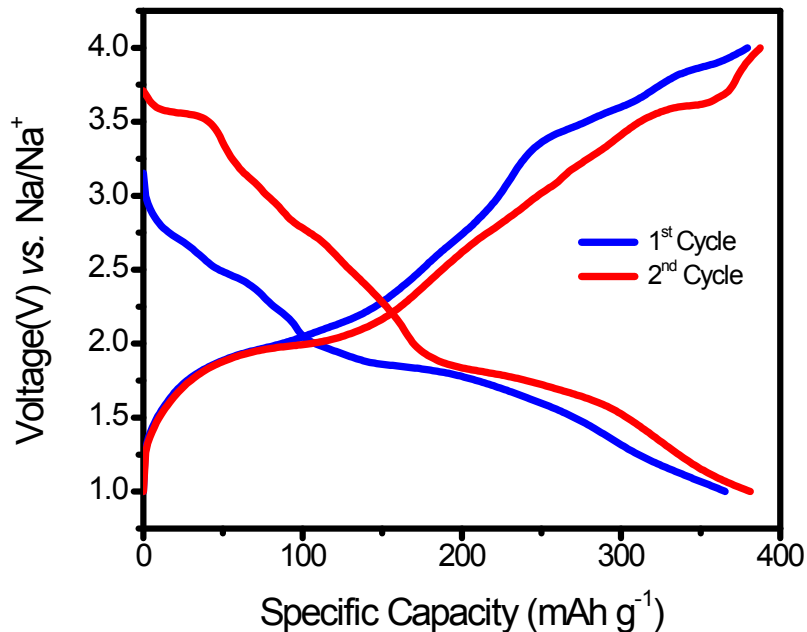


Fig. S8. Electrochemical performance of Zr-NH₄V₄O₁₀ over the potential window 1-4V at the current rate of 100 mA g⁻¹.

Table S3. Comparison of recent works on cathode materials for sodium ion battery with our Zr-NH₄V₄O₁₀.

Materials	Current Rate (mA g⁻¹)	Capacity (mAh g⁻¹)	Capacity Retention % (cycle number)
G-VOPO ₄ ³	0.05 C (8.33)	150	86 (50 th)
G-(NH ₄) _{0.19} V ₂ O ₅ ·0.44H ₂ O ⁴	20	208.9	67.73 (40 th)
α-NaV ₂ O ₅ ⁵	20	473	76.53 (2 nd)
Na ₃ V _{1.8} Al _{0.2} (PO ₄) ₃ ⁶	C/2	107	96 (60 th)
Fe-VO _x ⁷	100	184	80 (50 th)
NVONBs ⁸	50	125	65.6 (190 th)
Sponge-like V ₂ O ₅ ⁹	20	216	81 (20 th)
Zr-NH₄V₄O₁₀ Present work	200	275	87 (50th)

Table S4. Comparison of recent works on the sodium ion full cell with our Zr-NH₄V₄O₁₀ || H-Na₂Ti₃O₇ full cell.

Full cell Configuration	Voltage	Rate (mA g⁻¹)	Specific Capacity (mAh g⁻¹)	Energy Density (Wh kg⁻¹)	Capacity Retention
Na ₂ Ti ₃ O ₇ //VOPO ₄ ¹⁰	2.9 V	10 (0.1 C)	114	220	92.4% (100 th)
H-Na ₂ Ti ₃ O ₇ //Na _{2/3} (Ni _{1/3} Mn _{2/3})O ₂ ¹¹	2.7 V	1 C	182	490 (anode base)	(100 th)
XXX (FARADION)	3 V	---	162	486	---
TiO ₂ //Na ₂ V ₂ O ₅ ¹²	2.3 V	1 C	118 mAh g ⁻¹	271	76% (350 th)
Fe ₂ O ₃ NiO//Na ₃ V ₂ (PO ₄) ₃ ¹³	1.8 V	C/2	100 mAh g ⁻¹	180	80% (30 th)
Fe ₃ O ₄ //Na ₂ P ₂ O ₇ ¹⁴	2.28 V	0.1 C	93 mAh g ⁻¹	203	93.3% (100 th)
TiO ₂ NT//NaLi _{0.2} Ni _{0.25} Mn _{0.75} O _X ¹⁵	1.8 V	11 mA g ⁻¹	78 mAh g ⁻¹	104	---
H-Na₂Ti₃O₇//Zr-NH₄V₄O₁₀ (Present Work)	2.41 V	200	194	467	95% (200th)

XXX: FARADION (Not mention of the chemistry of the battery material)

All the full cell capacity was calculated based on active cathode materials weight.

For storage devices, the fundamental requirement is high energy density (Wh kg^{-1}) material which can be achieved by 1) high potential (V) and 2) high capacity (mAh g^{-1}). Though the nominal voltage of ammonium vanadate is ~ 1.9 V, it has high specific capacity ~ 345 mAh g^{-1} which gives overall energy density (gravimetric) ~ 655.5 Wh kg^{-1} . Similarly, for the full cell, the nominal voltage is ~ 1.68 V and specific capacity ~ 202 mAh g^{-1} which implies 339 Wh kg^{-1} (cathode limited cell). The energy density of various commercial materials is given Table S3. Based on the data presented above, ammonium vanadate based cathode is compatible with commercial lithium ion batteries materials. Though the nominal full cell voltage is ~ 1.68 V, still for high voltage applications these low voltage cells can be connected in series to achieve the desired voltage.

Table S5. Comparison of recent commercial materials with our $\text{Zr-NH}_4\text{V}_4\text{O}_{10}$ cathode materials.

Cathode Materials	Capacity (mAh g^{-1})	Nominal Potential (V)	Energy Density Wh kg^{-1}
Li_xCoO_2	155	3.7	573
LiFePO_4	170	3.2	544
$\text{Zr-NH}_4\text{V}_4\text{O}_{10}$	345	1.9	655

Note: The calculation is based on cathode material not for full cell configuration):

References

- 1 A. Sarkar, S. Sarkar, T. Sarkar, P. Kumar, M. D. Bharadwaj and S. Mitra, *ACS Appl. Mater. Interfaces*, 2015, **7**, 17044–17053.
- 2 H. M. Barkholtz, J. R. Gallagher, T. Li, Y. Liu, R. E. Winans, T. Miller, D. Liu and T. Xu, *Chemical Rev.*, 2016, **28**, 2267–2277.
- 3 G. He, W. H. Kan and A. Manthiram, *Chem. Mater.*, 2016, 682–688.

- 4 H. Fei, H. Li, Z. Li, W. Feng, X. Liu and M. Wei, *Dalton Transactions*, 2014, 16522–16527.
- 5 P. Liu, D. Zhou, K. Zhu, Q. Wu, Y. Wang, G. Tai, W. Zhang and Q. Gu, *Nanoscale*, 2016, **8**, 1975–1985.
- 6 M. J. Aragón, P. Lavela, R. Alcántara and J. L. Tirado, *Electrochim. Acta*, 2015, **180**, 824–830.
- 7 Q. Wei, Z. Jiang, S. Tan, Q. Li, L. Huang, M. Yan, L. Zhou, Q. An and L. Mai, *ACS Appl. Mater. Interfaces*, 2015, **7**, 8211–18217.
- 8 S. Yuan, Y. Liu, D. Xu, D. Ma, S. Wang and X. Yang, *Adv. Sci.*, 2015, **2**, 11400018.
- 9 K. Zhu, C. Zhang, S. Guo, H. Yu, K. Liao and G. Chen, *chemelectrochem*, 2015, **210093**, 1660–1664.
- 10 S. Guo, H. Yu, P. Liu, Y. Ren, T. Zhang, M. Chen, M. Ishida and H. Zhou, *Energy Environ. Sci.*, 2015, **8**, 1237–1244.
- 11 S. Fu, J. Ni, Y. Xu, Q. Zhang and L. Li, *Nano Energy*, 2016, **16**, 4544–4551.
- 12 S. Tepavcevic, *Electrochem. Soc.*, 2013, **6**, 2565.
- 13 M. C. López, M. J. Aragón, G. F. Ortiz, P. Lavela and R. Alcántara, *Chem. a Eur. J.*, 2015, **2**, 14879–14885.
- 14 J. Ming, H. Ming, W. Yang, W. Kwak and J. Park, *RSC Adv.*, 2015, **5**, 8793–8800.
- 15 H. Xiong, M. D. Slater, M. Balasubramanian, C. S. Johnson and T. Rajh, *J. Phys. Chem. Chem. Lett.*, 2011, **2**, 2560–2565.